Journal of Sound and Vibration (2001) **240**(4), 623–636
doi:10.1006/jsvi.2000.3265, available online at http://www.idealibrary.com on IDEAL®

SENSITIVITY ANALYSES OF SENSOR LOCATIONS FOR VIBRATION CONTROL AND DAMAGE DETECTION OF THIN-PLATE SYSTEMS

Y. Y. Li and L. H. Yam

Department of Mechanical Engineering, The Hong Kong Polytechnic University, Hung Hom, Kowloon, Hong Kong SAR, People's Republic of China. E-mail: mmlhyam@polyu.edu.hk

(*Received* 18 *January* 2000, *and in final form* 4 *July* 2000)

This paper addresses the sensitivity problem of sensor locations for vibration control and damage detection of thin-plate systems with parameter variation or noise. For vibration control, the technique for robust determination of sensor locations is presented. Based on the spectral condition number of the Hankel matrix, the optimal sensor locations (OSLs) can be determined, and the effect of noise on the OSLs is investigated using the matrix perturbation theory. For damage detection, the damage locations can be determined using the damage index β derived from the curvature modes. The sensitivity analysis of sensor locations on the detection result for systems with parameter variation is presented. Some experiments are carried out to verify the effectiveness of the proposed method.

1. INTRODUCTION

The problem of sensor locations is crucial for system identification [1–4], active vibration control [5–7] and damage detection [8, 9], which require accurate measurement of the responses of the structure. Many methods, such as the minimal energy principle, mode shape independent principle, degree of observability, Fisher information matrix, etc. have been developed for the determination of sensor locations in many contributions [10–13].

In engineering practice, the measured data are always inaccurate because of the existence of parameter variation or noise. In such cases, a question arises naturally, i.e., are the conventional studies on the determination of sensor locations from these measured data still valid, or under what conditions will the determined locations be insensitive to parameter variation or noise during system identification, vibration control or damage detection?

A survey of the literature shows that the sensitivity analysis of sensor locations for system identification has been investigated intensively [2, 14–16]. Kirkegaard and Brincker determined the OSLs for parametric identification of linear structural systems, and discussed the influence of noise on these OSLs [2]. Kammer studied the effects of noise on sensor placement for on-orbit modal identification of large space structures [14]. Fadale *et al.* suggested that erroneous estimates of the parameters can be ameliorated by placing the sensors at points of maximum sensitivity [15].

However, very few papers have addressed the problems of the sensitivity analysis of sensor locations for vibration control or damage detection. Ma *et al.* investigated the effects of parameter variation on vibration control of beam structures, and established the relationship between robust control and the determination of sensor locations [17]. As for the robust determination of sensor locations for the vibration control of thin-plate systems,

0022-460X/01/090623 + 14 $35.00/0

the effect of noise on the OSLs, and the sensitivity analysis of sensor locations to parameter variation for damage detection, no constructive results have been reported.

The aim of this paper is to study these problems systematically. The structure of this paper is organized as follows. In section 2, the condition for robust determination of sensor location for the vibration control of thin-plate systems with parameter variation is derived, the index for optimal assignment of locations is presented, and the method for analyzing the influence of noise on the OSLs is given. The sensitivity analysis of sensor locations for damage detection and the effect of parameter variation are discussed in section 3. In section 4, the experimental investigations are described and analyzed. Finally, conclusions are drawn.

2. SENSITIVITY ANALYSIS OF SENSOR LOCATIONS FOR VIBRATION CONTROL

2.1. FORMULATION OF THE PROBLEM

The differential equation of a thin plate subjected to control force $F \in \Re^s$ is given by

$$m_0(x, y)\frac{\partial^2 w(x, y, t)}{\partial t^2} + D_0\left(\frac{\partial^4 w(x, y, t)}{\partial x^4} + 2\frac{\partial^4 w(x, y, t)}{\partial x^2\,\partial y^2} + \frac{\partial^4 w(x, y, t)}{\partial y^4}\right) + c_0(x, y)\frac{\partial w(x, y, t)}{\partial t} = F(x, y, t), \quad (0 < x \leqslant a, 0 < y \leqslant b), \tag{1}$$

where $w(x, y, t)$, $m_0(x, y)$, D_0 and c_0 are the transverse deflection, the mass per unit area, the flexural rigidity and the damping coefficient of the thin plate respectively. a and b are the dimensions of the plate. Based on the mode superposition theory, the transverse deflection $w(x, y, t)$ can be expressed as

$$w(x, y, t) = \sum_{i=1}^{m}\sum_{j=1}^{n}\phi_{ij}(x, y)\eta_{ij}(t), \tag{2}$$

where $\eta_{ij}(t)$ and $\phi_{ij}(x, y)$ are the ijth modal co-ordinate and shape function respectively. Assuming that the outputs $\mathbf{y}(t)$ are a set of l displacement signals, with the transformation $\mathbf{Q}(t) = \{\eta(t)^{\mathrm{T}}\ \dot{\eta}(t)^{\mathrm{T}}\}^{\mathrm{r}}$, the system can be written in the state-space form as

$$\dot{\mathbf{Q}}(t) = \mathbf{A}\mathbf{Q}(t) + \mathbf{B}\mathbf{U}(t), \qquad \mathbf{y}(t) = \mathbf{C}\mathbf{Q}(t), \tag{3}$$

where $\mathbf{U}(t)$ is the vector of control force F,

$$\mathbf{A} = \begin{bmatrix} 0 & & 1 & & & \\ & \ddots & & \ddots & & \\ & & 0 & & & 1 \\ -\omega_{11}^2 & & & -2\zeta_{11}\omega_{11} & & \\ & \ddots & & & \ddots & \\ & & -\omega_{mn}^2 & & & -2\zeta_{mn}\omega_{mn} \end{bmatrix},$$

$$\mathbf{B} = \frac{1}{m_0 ab}\begin{bmatrix} 0 & \cdots & 0 \\ \cdots & \cdots & \cdots \\ 0 & \cdots & 0 \\ \phi_{11}(x_{l+1}, y_{l+1}) & \cdots & \phi_{11}(x_{l+s}, y_{l+s}) \\ \cdots & \cdots & \cdots \\ \phi_{mn}(x_{l+1}, y_{l+1}) & \cdots & \phi_{mn}(x_{l+s}, y_{l+s}) \end{bmatrix},$$

$$\mathbf{C} = \begin{bmatrix} \phi_{11}(x_1, y_1) & \cdots & \phi_{mn}(x_l, y_l) & 0 & \cdots & 0 \\ & \cdots & \cdots & \cdots & & \\ \phi_{11}(x_1, y_1) & \cdots & \phi_{mn}(x_l, y_l) & 0 & \cdots & 0 \end{bmatrix}. \tag{4}$$

Let ζ_{ij} and ω_{ij} denote the damping ratio and the natural frequency of the ijth mode respectively. Conventionally, the sensor locations are determined using the measure of degree of observability based on the observability grammian $\mathbf{P}$, which is the solution of the Lyapunov equation [18, 19]

$$\mathbf{A}^{\mathrm{T}}\mathbf{P} + \mathbf{P}\mathbf{A} + \mathbf{C}^{\mathrm{T}}\mathbf{C} = 0. \tag{5}$$

However, when the parameters $(\omega_{ij}, \zeta_{ij})$ of $\mathbf{A}$ vary in the region $\{\zeta_{ij}, \omega_{ij} | \zeta_{ij} \subset [\zeta_{ij} - \Delta\zeta_{ij}\ \zeta_{ij} + \Delta\zeta_{ij}], \omega_{ij} \subset [\omega_{ij} - \Delta\omega_{ij}\ \omega_{ij} + \Delta\omega_{ij}], 1 \leqslant i \leqslant m, 1 \leqslant j \leqslant n\}$, it is impossible to solve $\mathbf{P}$ in equation (5) determinatively. As a result, it will be difficult to locate sensors at the proper positions. For this reason, it is necessary to find a way to determine the sensor locations robustly for the vibration control of thin-plate systems with parameter variation.

2.2. CONDITION FOR ROBUST DETERMINATION OF SENSOR LOCATIONS

For an uncertain thin plate with variable parameter feedback control $\mathbf{U}(t) = \mathbf{K}(r_o)Q(t)$[20] (see Figure 1), the Laplace transformation of the responses $\mathbf{y}(t)$ can be expressed as

$$\mathbf{y}(\omega) = [\mathbf{I}_{l\times l} + \tilde{\mathbf{G}}(\omega)\cdot\mathbf{K}(r_o)]^{-1}\tilde{\mathbf{G}}(\omega)\cdot\mathbf{U}_{ref}(\omega), \tag{6}$$

where $\mathbf{U}_{ref}(\omega)$ and r_o are the reference input and the adjustable parameter respectively. $\tilde{\mathbf{G}}(\omega)$ is the transfer function under the parameter variation. Denote the real part of the diagonal element of matrix $(\cdot)$ as $\Re_e\{diag(\cdot)\}$; if the condition

$$J_p = \Re_e\{diag[\tilde{\mathbf{G}}(\omega)\cdot\mathbf{K}(r_o)]\}_p \gg 1 \quad (p = 1, \ldots, l) \tag{7}$$

is satisfied, equation (6) can be rewritten as

$$\mathbf{y}(\omega) \approx \mathbf{K}(r_o)^{-1}\cdot\mathbf{U}_{ref}(\omega). \tag{8}$$

The above derivation shows that with the constraint of $J_p \gg 1$, the responses $\mathbf{y}(\omega)$ will depend on $\mathbf{K}(r_o)$ and $\mathbf{U}_{ref}(\omega)$, and are insensitive to parameter variation. Since the elements of matrix $\tilde{\mathbf{G}}(\omega)$ are related to $\tilde{\phi}_{ij}(x_p, y_p)$, in which (x_p, y_p) is a set of sensor locations to be determined, there exists a certain implication for determining $\tilde{\phi}_{ij}(x_p, y_p)$ to make equation (7) valid. Without loss of generality, separate the pqth complex element of $[\mathbf{K}(r_o)]_{s\times l}$ as

$$k_{pq}(r_o) = \Re_e[k_{pq}(r_o)] + j\Im_m[k_{pq}(r_o)], \tag{9}$$

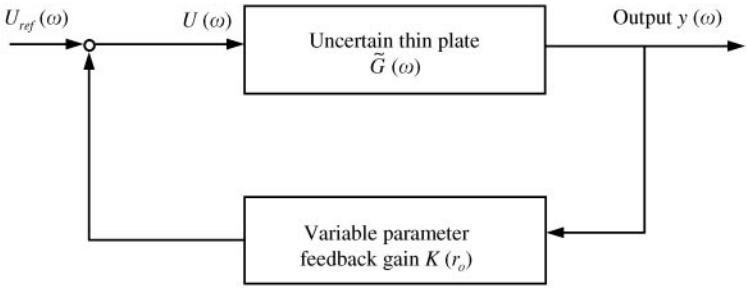

Figure 1. Block diagram of the VPFC system.

J_p in equation (7) becomes

$$J_p = \sum_{q=1}^{s} \sum_{i=1}^{m} \sum_{j=1}^{n} \tilde{\phi}_{ij}(x_p, y_p)\tilde{\phi}_{ij}(x_{l+k}, y_{l+k}) \frac{\{(\tilde{\omega}_{ij}^2 - \omega^2)\Re_e[k_{pq}(r_o)] + 2\tilde{\zeta}_{ij}\tilde{\omega}_{ij}\omega\Im_m[k_{pq}(r_o)]\}}{(\tilde{\omega}_{ij}^2 - \omega^2)^2 + 4\tilde{\zeta}_{ij}^2\tilde{\omega}_{ij}^2\omega_{ij}^2}. \tag{10}$$

Denote $\tilde{\phi}_{ij}(x_p, y_p) = \tilde{\phi}_{ij}(x, y)|_{\substack{x=x_p \\ y=y_p}}$ and express $\tilde{\phi}_{ij}(x, y)$ in the form

$$\tilde{\phi}_{ij}(x, y) = \sum_{d=1}^{n_o} f_{d,ij}(x, y)\tilde{c}_{d,ij}, \tag{11}$$

where $f_{d,ij}(x, y)$ is a function of (x, y), which is determined by the boundary conditions. For example, for the clamped edges, $n_a = 4$, and

$$\begin{aligned}
f_{1,ij}(x, y) &= [\sin(\alpha_i x/a) - \sinh(\alpha_i x/a)][\sin(\beta_j y/b) - \sinh(\beta_j y/b)], \\
f_{2,ij}(x, y) &= [\sin(\alpha_i x/a) - \sinh(\alpha_i x/a)][\cos(\beta_j y/b) - \cosh(\beta_j y/b)], \\
f_{3,ij}(x, y) &= [\cos(\alpha_i x/a) - \cosh(\alpha_i x/a)][\sin(\beta_j y/b) - \sinh(\beta_j y/b)], \\
f_{4,ij}(x, y) &= [\cos(\alpha_i x/a) - \cosh(\alpha_i x/a)][\cos(\beta_j y/b) - \cosh(\beta_j y/b)] \\
&(\alpha_i = (2i + 1)\pi/2, \beta_j = (2j + 1)\pi/2)
\end{aligned} \tag{12}$$

and for the simply supported edges, $n_a = 1$, and

$$f_{1,ij}(x, y) = \sin(\alpha_i x/a)\sin(\beta_j y/b) \quad (\alpha_i = i\pi, \beta_j = j\pi) \tag{13}$$

$\tilde{c}_{d,ij}$ is the coefficient.

In order to make $J_p \gg 1$ valid, $\tilde{\phi}_{ij}(x, y) \to \max\{\tilde{\phi}_{ij}(x, y)\}|_{\substack{x=x_p \\ y=y_p}}$. That is, the sensors are assigned at those locations where the following conditions are satisfied:

$$\begin{aligned}
\frac{\partial\tilde{\phi}_{ij}(x, y)}{\partial x} &= \left[\frac{\partial f_{1,ij}(x, y)}{\partial x}, \cdots, \frac{\partial f_{n_a,ij}(x,y)}{\partial x}\right]\{\tilde{c}_{1,ij} \cdots \tilde{c}_{n_a,ij}\}^{\mathrm{T}} = 0, \\
\frac{\partial\tilde{\phi}_{ij}(x, y)}{\partial y} &= \left[\frac{\partial f_{1,ij}(x, y)}{\partial y}, \cdots, \frac{\partial f_{n_a,ij}(x,y)}{\partial y}\right]\{\tilde{c}_{1,ij} \cdots \tilde{c}_{n_a,ij}\}^{\mathrm{T}} = 0.
\end{aligned} \tag{14}$$

Obviously, one solution of equation (14) is that

$$\begin{aligned}
\left[\frac{\partial f_{1,ij}(x, y)}{\partial x}, \cdots, \frac{\partial f_{n_a,ij}(x,y)}{\partial x}\right] &= [0]_{1\times n_a}, \\
\left[\frac{\partial f_{1,ij}(x, y)}{\partial y}, \cdots, \frac{\partial f_{n_a,ij}(x,y)}{\partial y}\right] &= [0]_{1\times n_a}.
\end{aligned} \tag{15}$$

The above analysis shows that:

- when the sensors are assigned at the locations determined according to equation (15), the condition equation (7) holds. That is to say, the responses will be robust to parameter variation for vibration control;
- from equation (15), the determination of sensor locations relates to function $f_{d,ij}(x, y)$ (or mode shape $\tilde{\phi}_{ij}(x, y)$), and is independent of modal frequencies ω_{ij} and modal dampings ζ_{ij};
- the satisfied locations are near the points where the extreme amplitudes for the dominant modes occur;
- the number of candidate locations is larger than the number of sensors to be placed, which is always set as the number of modes to be monitored.

2.3. CRITERION FOR THE OSLs

Having identified the sensor locations, the problem will be which criterion among the combinations of all possible sensor locations to adopt in order to select an optimal set effectively, such that the measured data will give desirable results for achieving a better estimation of structural states. Our strategy is to monitor and compare the spectral condition number (SCN) of the Hankel matrix. It is shown that there are OSLs, for which the SCN is minimized. Constructing a Hankel matrix by overlapping length L subsets of $\mathbf{y}_k$,

$$\mathbf{H}_{k-1}(r,l) = \begin{bmatrix} \mathbf{y}_k & \mathbf{y}_{k+1} & \cdots & \mathbf{y}_{k+L-1} \\ \mathbf{y}_{k+1} & \mathbf{y}_{k+2} & \cdots & \mathbf{y}_{k+L} \\ \vdots & \vdots & \ddots & \vdots \\ \mathbf{y}_{k+r-1} & \mathbf{y}_{k+r} & \cdots & \mathbf{y}_{k+r+L-2} \end{bmatrix}_{rl \times L} \tag{16}$$

and rl is chosen larger than the expected model order. Define the SCN as

$$\kappa(\mathbf{H}_{k-1}) = \| \mathbf{H}_{k-1} \| \, \| \mathbf{H}_{k-1}^{+} \|, \tag{17}$$

where the superscript " + " denotes pseudo-inverse. The criterion is to locate sensors at those positions where $\kappa(\mathbf{H}_{k-1})$ reaches its minimum, so as to achieve the best control effect.

2.4. EFFECT OF NOISE ON THE OSLs

An important factor that affects the sensor locations is the signal-to-noise ratio (SNR). It is known that the precision of a measurement is limited by the SNR of the measured data. For this reason, the problem of interest herein can now be stated as follows: when the measured data used for SCN analysis are contaminated by noise, under what conditions will the OSLs remain optimal?

Consider that the measured responses polluted by noise are given as

$$\tilde{\mathbf{y}}_k = \mathbf{y}_k + \upsilon_k, \tag{18}$$

where $\upsilon_k = \{\upsilon_{1,k}, \ldots, \upsilon_{l,k}\}^{\mathrm{T}}$ is the vector of noise. Correspondingly, the perturbed Hankel matrix $\tilde{\mathbf{H}}_{k-1}$ can be expressed as

$$\tilde{\mathbf{H}}_{k-1} = \mathbf{H}_{k-1} + \mathbf{v}_{k-1}, \tag{19}$$

$\mathbf{v}_{k-1}$ is a matrix of $v_k, \ldots, v_{k+r+s-1}$. According to equation (17), $\kappa(\mathbf{H}_{k-1})$ is replaced by

$$\kappa(\tilde{\mathbf{H}}_{k-1}) = \|\tilde{\mathbf{H}}_{k-1}\| \, \|\tilde{\mathbf{H}}_{k-1}^{+}\|. \tag{20}$$

In order to reveal the relationship between $\kappa(\tilde{\mathbf{H}}_{k-1})$ and $\kappa(\mathbf{H}_{k-1})$, the relationship between $\|\tilde{\mathbf{H}}_{k-1}^{+}\|$ and $\|\mathbf{H}_{k-1}^{+}\|$ is investigated using the matrix perturbation theory in advance.

Lemma [21]. $\forall \exists \mathbf{H}_{k-1}, \ \tilde{\mathbf{H}}_{k-1} \in C^{m\times n}$, *if* $rank(\tilde{\mathbf{H}}_{k-1}) = rank(\mathbf{H}_{k-1})$ *and* $\varepsilon = \|\mathbf{H}_{k-1}^{+}\| \, \|\mathbf{v}_{k-1}\| < 1$, *then*

$$\|\tilde{\mathbf{H}}_{k-1}^{+} - \mathbf{H}_{k-1}^{+}\| / \|\mathbf{H}_{k-1}^{+}\| \leqslant \frac{\mu\varepsilon}{(1-\varepsilon)}, \quad \mu = \begin{cases} (1+\sqrt{5})/2 & rank(\mathbf{H}_{i-1}) < min(lr, (L+1)/2), \\ \sqrt{2} & rank(\mathbf{H}_{i-1}) = min(lr, (L+1)/2). \end{cases} \tag{21}$$

Equation (21) gives the upper perturbation bound of $\tilde{\mathbf{H}}_{k-1}^{+}$. From equation (21), one obtains

$$\|\tilde{\mathbf{H}}_{k-1}^{+}\| \leqslant \left(1 + \frac{\mu\varepsilon}{(1-\varepsilon)}\right) \|\mathbf{H}_{k-1}^{+}\|. \tag{22}$$

Assume that the signals and the noises are statistically independent of each other. Equation (20) can then be rewritten as

$$\begin{aligned} \kappa(\tilde{\mathbf{H}}_{k-1}) &= \|\mathbf{H}_{k-1} + \mathbf{v}_{k-1}\| \cdot \|\tilde{\mathbf{H}}_{k-1}^{+}\| \\ &\approx \alpha_{k,1}\left(1 + \frac{\mu\varepsilon}{(1-\varepsilon)}\right)\kappa(\mathbf{H}_{k-1}) \quad (0 < \alpha_{k,1} \leqslant 1). \end{aligned} \tag{23}$$

Equation (23) implies the connection between $\kappa(\mathbf{H}_{k-1})$ from noise-free data and $\kappa(\tilde{\mathbf{H}}_{k-1})$ from noisy data. It is found that the SCN of $\kappa(\tilde{\mathbf{H}}_{k-1})$ is proportional to $\kappa(\mathbf{H}_{k-1})$, i.e., $\kappa(\tilde{\mathbf{H}}_{k-1}) \propto \kappa(\mathbf{H}_{k-1})$, and only a small perturbation will be performed on $\tilde{\mathbf{H}}_{k-1}^{+}$. Based on this fact, the following proposition is immediate.

Proposition. *The sensor locations determined in noise-free cases are insensitive to noise if and only if the conditions*:

(*a*) $rank(\tilde{\mathbf{H}}_{k-1}) = rank(\mathbf{H}_{k-1})$; *and* (*b*) $\|\mathbf{v}_{k-1}\| \to 0 \left(or \ \frac{\mu\varepsilon}{(1-\varepsilon)} \approx 0(\varepsilon) \right)$ *are satisfied.*

3. SENSITIVITY ANALYSIS OF SENSOR LOCATIONS FOR DAMAGE DETECTION

Damage in thin-plate systems results in changes in their identified modal parameters, which have been used to assess the integrity of the structures extensively. Usually, the vibration signatures, such as natural frequency, mode shape, etc. are the sensitive indices, which can provide an indication of the extension of the cracked zones in structures [22–24]. In recent years, the techniques of utilizing mode shape data have been developed and used extensively for damage detection and severity estimation of structures [25, 26]. As is known, when the damage occurs, the curvature mode shapes of the systems will be changed [27, 28]. Based on this fact, the relative change in curvature mode is adopted as the index to locate damage for thin-plate systems.

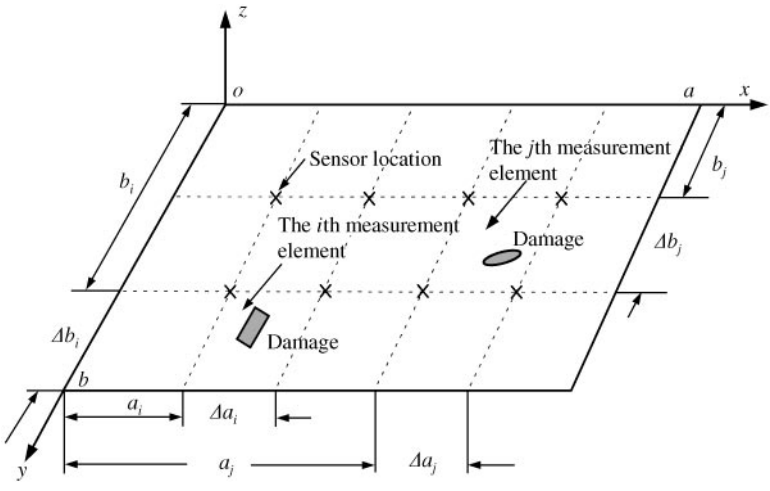

Figure 2. Schematic diagram of a thin-plate with damages.

Denote the damage index β_{p_r} as (see Figure 2)

$$\beta_{p_r} = \sum_{i=1}^{m}\sum_{j=1}^{n} \frac{\int_{b_{p_r}}^{b_{p_r}+\Delta b_{p_r}} \int_{a_{p_r}}^{a_{p_r}+\Delta a_{p_r}} ([(\phi_{ij})''_{da}(x,y)]^2 - [(\phi_{ij})''(x,y)]^2)\,\mathrm{d}x\,\mathrm{d}y}{\sum_{p_r=1}^{n_c} \int_{b_{p_r}}^{b_{p_r}+\Delta b_{p_r}} \int_{a_{p_r}}^{a_{p_r}+\Delta a_{p_r}} [(\phi_{ij})''(x,y)]^2\,\mathrm{d}x\,\mathrm{d}y}$$

$$(p_r = 1, \ldots, n_c), \tag{24}$$

where $(\phi_{ij})''_{da}(x, y)$ and $(\phi_{ij})''(x, y)$ are the second derivatives of the ijth normalized mode shape corresponding to the damaged and intact structures respectively. n_c is the number of measured elements. Similar to equation (11),

$$(\phi_{ij})''_{da}(x,y) = \sum_{d=1}^{n_a} (c_{d,ij})_{da} f''_{d,ij}(x,y) \quad (\phi_{ij})''(x,y) = \sum_{d=1}^{n_a} c_{d,ij} f''_{d,ij}(x,y). \tag{25}$$

Using the Cauchy–Schwartz inequality, one obtains

$$\left[\sum_{d=1}^{n_a} (c_{d,ij})_{da} f''_{d,ij}(x,y)\right]^2 \leqslant \sum_{d=1}^{n_a} [(c_{d,ij})_{da}]^2 \sum_{d=1}^{n_a} [f''_{d,ij}(x,y)]^2, \tag{26}$$

$$\left[\sum_{d=1}^{n_a} (c_{d,ij}) f''_{d,ij}(x,y)\right]^2 \leqslant \sum_{d=1}^{n_a} [(c_{d,ij})]^2 \sum_{d=1}^{n_a} [f''_{d,ij}(x,y)]^2. \tag{27}$$

Denoting

$$\left[\sum_{d=1}^{n_a} (c_{d,ij})_{da} f''_{d,ij}(x,y)\right]^2 = (\gamma_{da})_{ij} \sum_{d=1}^{n_a} [(c_{d,ij})_{da}]^2 \sum_{d=1}^{n_a} [f''_{d,ij}(x,y)]^2, \quad 0 < (\gamma_{da})_{ij} \leqslant 1, \tag{28}$$

$$\left[\sum_{d=1}^{n_a} (c_{d,ij}) f''_{d,ij}(x,y)\right]^2 = \gamma_{ij} \sum_{d=1}^{n_a} [(c_{d,ij})]^2 \sum_{d=1}^{n_a} [f''_{d,ij}(x,y)]^2, \quad 0 < \gamma_{ij} \leqslant 1 \tag{29}$$

and

$$g_{ij} = \int_{b_{p_r}}^{b_{p_r}+\Delta b_{p_r}} \int_{a_{p_r}}^{a_{p_r}+\Delta a_{p_r}} \left(\sum_{d=1}^{n_a} [f''_{d,ij}(x, y)]^2 \right) \mathrm{d}x\, \mathrm{d}y \Bigg/ \sum_{p_r=1}^{n_c} \int_{b_{p_r}}^{b_{p_r}+\Delta b_{p_r}} \int_{a_{p_r}}^{a_{p_r}+\Delta a_{p_r}} \left(\sum_{d=1}^{n_a} [f''_{d,ij}(x, y)]^2 \right) \mathrm{d}x\, \mathrm{d}y, \tag{30}$$

β_{p_r} can be expressed as follows by substituting equations (25, 28–30) into equation (24),

$$\beta_{p_r} = \sum_{i=1}^{m} \sum_{j=1}^{n} g_{ij} \left((\gamma_{da})_{ij} \sum_{d=1}^{n_a} [(c_{d,ij})_{da}]^2 \Big/ \gamma_{ij} \sum_{d=1}^{n_a} [(c_{d,ij})]^2 - 1 \right). \tag{31}$$

It can be concluded that for the intact case, $\beta_{p_r} = 0$, while for the damaged case, $\beta_{p_r} \neq 0$ ($p_r = 1, \ldots, n_c$). Since, at damaged areas, differences of the curvature mode shapes between the intact and damaged structures are significant, damage locations can be determined at those positions where the peaks of β_{p_r} occur.

When a small variation of the system's parameters is taken into account, the following expressions will be true after some algebraic manipulations. The analysis of the influence of parameter variation on the damage detection results in

$$[(\tilde{\phi}_{ij})''_{da}(x, y)]^2 = (\gamma_{da})_{ij} \sum_{d=1}^{n_a} (\eta_{1,d})^2 \sum_{d=1}^{n_a} [(c_{d,ij})_{da}]^2 \sum_{d=1}^{n_a} [f''_{d,ij}(x, y)]^2, \tag{32}$$

$$[(\tilde{\phi}_{ij})'' x, y]^2 = \gamma_{ij} \sum_{d=1}^{n_a} (\eta_{2,d})^2 \sum_{d=1}^{n_a} [(c_{d,ij})]^2 \sum_{d=1}^{n_a} [f''_{d,ij}(x, y)]^2, \tag{33}$$

where $\eta_{1,d}$ and $\eta_{2,d}$ are the modified coefficients. Let

$$\eta = \sum_{d=1}^{n_a} (\eta_{1,d})^2 \Big/ \sum_{d=1}^{n_a} (\eta_{2,d})^2, \tag{34}$$

the damage index β_{p_r} under parameter variation be rewritten as

$$\begin{aligned} \tilde{\beta}_{p_r} &= \sum_{i=1}^{m} \sum_{j=1}^{n} g_{ij} \left((\gamma_{da})_{ij} \sum_{d=1}^{n_a} (\eta_{1,d})^2 \sum_{d=1}^{n_a} [(c_{d,ij})_{da}]^2 \Big/ \gamma_{ij} \sum_{d=1}^{n_a} (\eta_{2,d})^2 \sum_{d=1}^{n_a} [(c_{d,ij})]^2 - 1 \right) \\ &= \sum_{i=1}^{m} \sum_{j=1}^{n} \left(\eta \left((\gamma_{da})_{ij} \sum_{d=1}^{n_a} [(c_{d,ij})_{da}]^2 \Big/ \gamma_{ij} \sum_{d=1}^{n_a} [(c_{d,ij})]^2 - 1 \right) + (\eta - 1) \right) g_{ij} \\ &= \eta \beta_{p_r} + (\eta - 1) \sum_{i=1}^{m} \sum_{j=1}^{n} g_{ij}. \end{aligned} \tag{35}$$

Equation (35) shows the relationship between $\tilde{\beta}_{p_r}$ for the case with parameter variation and β_{p_r} for the nominal case. It can be found that the peaks of $\tilde{\beta}_{p_r}$ will also appear at those locations where the peaks of β_{p_r} appear, i.e., the damage locations detected for the nominal case are insensitive to small variations in the system's parameters.

4. EXPERIMENTAL VERIFICATION

Two experiments were carried out and their results are analyzed in this section. The first one is for the robust determination of sensor locations on vibration control and the influence of noise on the OSLs. The second one is for the sensitivity analysis of sensor locations on damage detection results for systems with parameter variation.

4.1. FOR VIBRATION CONTROL

Since damping is a property that is difficult to determine exactly, either experimentally or theoretically, it will be regarded as the variational parameter and taken to evaluate the robustness of the presented technique for determination of sensor location during vibration control.

4.1.1. *Experimental set-up and data acquisition*

The schematic diagram of the experimental set-up for a four-edge clamped thin steel plate with control is shown in Figure 3. The exciter (B&K 4809) was driven by the signal generated by a signal analyzer (B&K 3557) through a power amplifier (B&K 2706) to provide an excitation. The corresponding vibration responses were sensed by the accelerometers (B&K 4397) at different locations. Consider that low-frequency modes exert the dominant effects on systems' vibration control [29]; the highest frequency to be analyzed was set at 200 Hz. According to the sampling theorem, the sampling frequency should be more than twice the highest frequency of interest. The signals were therefore digitized at a rate of 2 kHz by A/D converter. A total of 3 K samples of time history were recorded for each sampling period by the signal analyzer. The data were then digitally filtered by an eighth order Butterworth filter with a corner frequency of 100 Hz to remove the high-frequency modes, and processed using the nominal realization parameters $l = 7$, $r = 5$ and $l = 100$, in which l depends on the available sensor numbers, rl is more than twice the model order and L should be larger than rl. It should be pointed out that the proper selection of parameters (r, L) is important for obtaining desirable results and avoiding a large calculation effort.

As is known, the accuracy of the experimental results is related to the quality of the measured data. In order to improve the quality of the measured data:

- sufficient care is taken during the data sampling operation, so that aliasing effects can be restricted to a high-frequency band far beyond the range of interest;
- "Ensemble averaging" is adopted during the measurement process to maximize SNR;

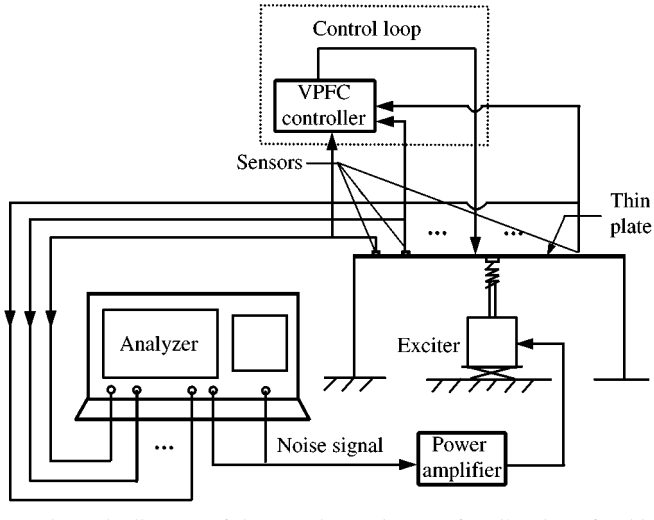

Figure 3. Schematic diagram of the experimental set-up for vibration of a thin plate.

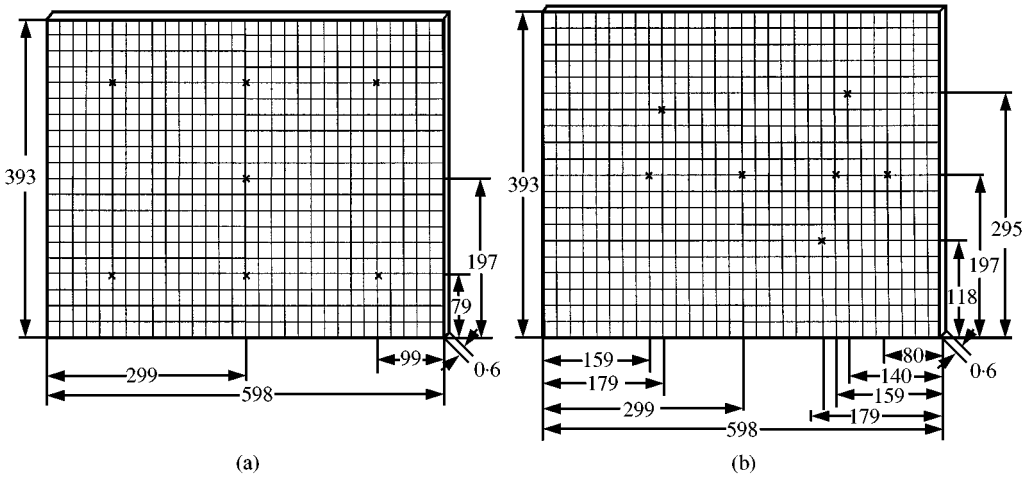

Figure 4. Two combinations of sensor locations: ×, sensor location (unit: mm).

- the stinger with low transverse and high axial stiffness is superior to the over-stiff stinger, and extra filter and amplifier are used to minimize the effect of measurement noise.

4.1.2. *Analysis of results*

Figure 4 shows two different combinations of sensor locations for vibration control. Figure 4(a) represents the normal case, in which the sensor locations are assigned regularly, while Figure 4(b) represents the optimal case, in which the sensor locations are assigned with robustness (equation (15)). Since the control effect can be observed from the changes of amplitude H of frequency response function (FRF) at each natural frequency, i.e., a small amplitude H will be obtained when the sensors are placed at the OSLs, the performance index $J_j = (1/l)\sqrt{\sum_{i=1}^{l} (H_i(\omega_j))^2}$ is adopted for analysis, where $j = 1, \ldots, n_\omega$, n_ω is the number of natural frequencies of interest. The FRFs of each measurement point were recorded by an FFT analyzer. Figure 5 shows the experimental results of FRF and the index J_j ($l = 7$, $n_\omega = 9$ for $\omega \leqslant 200$). It can be seen that the J_j value of case (b) (Figure 4(b)) is smaller than that of case (a) (Figure 4(a)). This means that when the sensor locations are arranged according to the method of robust determination of sensor locations presented in this paper, better control effect can be achieved than with the conventional sensor location assignment

To investigate the influence of noise on the OSLs, the SCNs of different combinations of sensor locations for the noise-free case $\kappa(\mathbf{H}_{k-1})$ and the noisy case $\kappa(\tilde{\mathbf{H}}_{k-1})$ are calculated for comparison. In order to acquire the noisy data, random noise (white noise) was generated by the analyzer and exerted on the tested structure, and no filter was added to eliminate the influence of noise during data sampling. In this example, $rank(\tilde{\mathbf{H}}_{k-1}) = rank(\mathbf{H}_{k-1}) = 32$ and $\| \mathbf{v}_{k-1} \| = 0{\cdot}012 \approx 0$; thus, according to the proposition, the determined OSLs in noise-free cases should be insensitive to the noise. Twenty-four different combinations of sensor locations were tested. The curves of the SCN for the noise-free and noisy cases are plotted in Figure 6. It is clear that:

- the SCNs $\kappa(\tilde{\mathbf{H}}_{k-1})$ for the noisy case are larger than the SCNs $\kappa(\mathbf{H}_{k-1})$ for the noise-free case;
- for noise-free data, the curve reaches its minimal value ($[\kappa(\mathbf{H}_{k-1})]_{min} = 110{\cdot}3$) at point **a** (solid line), i.e., for that combination of sensors (case 11, the sensor locations are

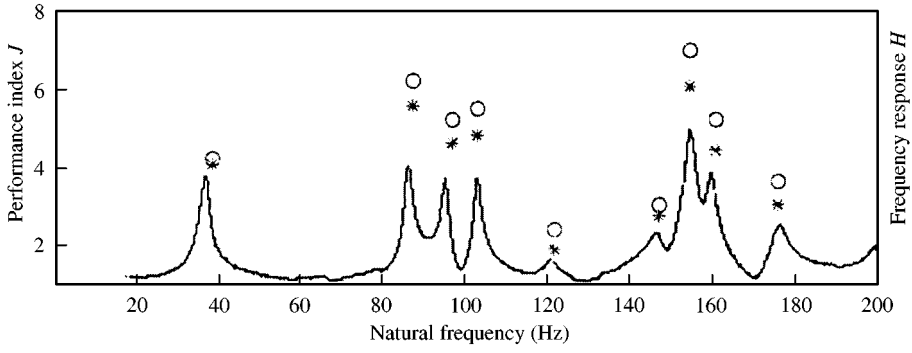

Figure 5. The result for performance index J: $*$, optimal location — Figure 4(b); $\bigcirc$, normal location — Figure 4(a).

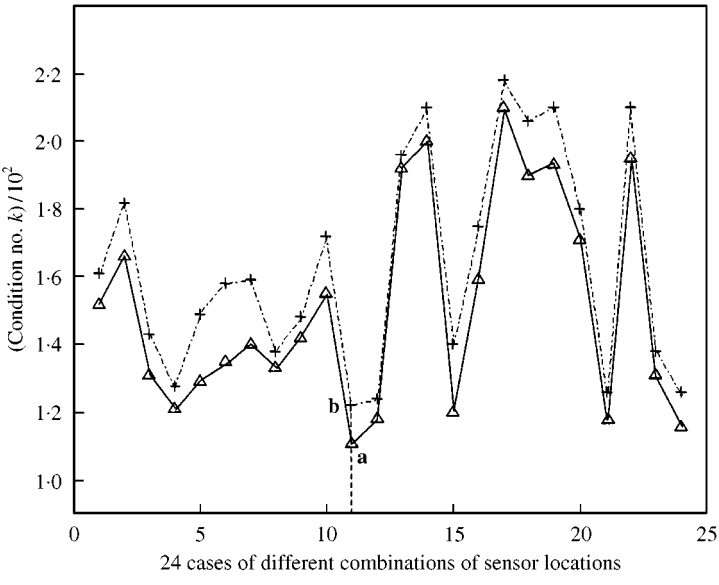

Figure 6. SCN versus different combinations of sensor locations: $+$, noisy data; Δ, noise-free data.

indicated in Figure 4(b)), the OSLs will be obtained. For noisy data, a similar result can be obtained at point **b** ($[\kappa(\tilde{\mathbf{H}}_{k-1})]_{min} = 122{\cdot}7$), i.e., the OSLs are the same for both noise-free and noisy cases. This shows that the experimental results are consistent with the theoretical analysis.

4.2. FOR DAMAGE DETECTION

To determine the damage location and analyze the sensitivity of sensor locations on the detection results for systems with parameter variation, the damage indices β_{p_r} and $\tilde{\beta}_{p_r}$ need to be computed. In this example, two thin steel plates with the same dimensions in length and width, but different thicknesses are taken to simulate the nominal system ($h = 0{\cdot}6$ mm) and the system with parameter variation ($h = 0{\cdot}7$ mm). The schematic diagram of the tested structure with damage is shown in Figure 7. There is a damaged area in element 8 for both plates.

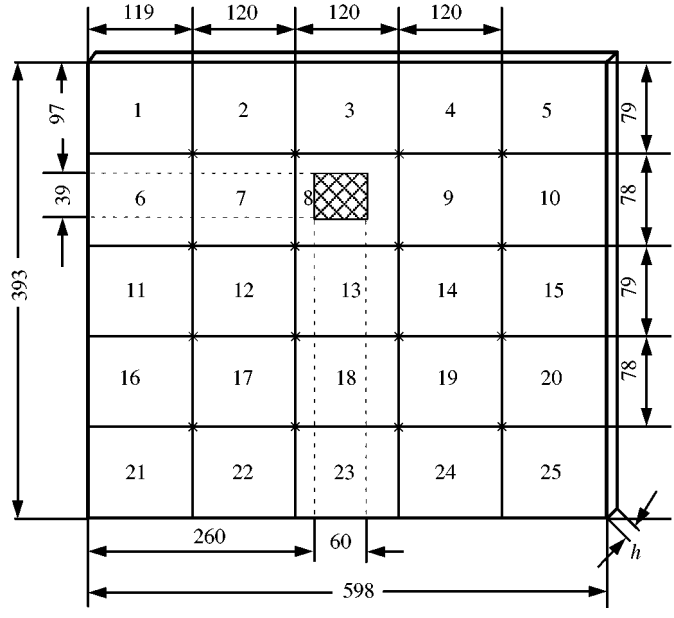

Figure 7. Tested structure for damage detection. *Case* 1: $h = 0{\cdot}6$; *case* 2: $h = 0{\cdot}7$ (unit: mm). ×, sensor location; ⊠, damaged area.

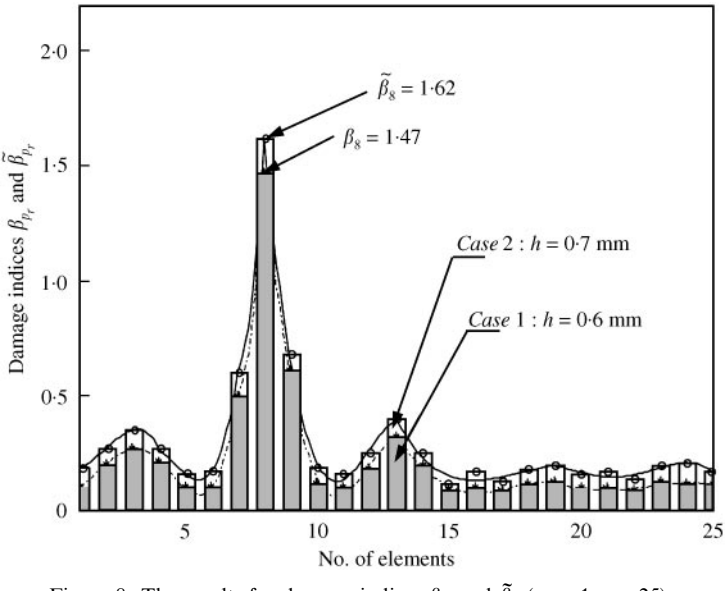

Figure 8. The results for damage indices β_{p_r} and $\tilde{\beta}_{p_r}$ ($p_r = 1, \ldots, 25$).

According to equations (24) and (35), the computations of β_{p_r} and $\tilde{\beta}_{p_r}$ and related to the curvature mode shapes of the nominal and variational systems, and the parameters mn and p_r. Here, $mn = 4$ and $p_r = 25$ are selected. The data of excitation and responses at 16 measurement points for the intact and damaged structures in the following two cases are sampled respectively: (1) with $h = 0{\cdot}6$ mm, (2) with $h = 0{\cdot}7$ mm, and then analyzed to give

the first four mode shapes and their curvature modes using the modal analysis software and mathematical processing. Figure 8 shows the results of β_{p_r} and $\tilde{\beta}_{p_r}$. It can be seen that:

- for the nominal system ($h = 0{\cdot}6$ mm), $\beta_{p_r} \neq 0$. β_{p_r} achieves its maximum at the damaged area (element 8), i.e., $\beta_8 = 1{\cdot}47$; in contrast, at the undamaged area, β_{p_r} is at a low level. This means that the damage index derived from curvature mode shapes is effective in damage detection;
- for the system with parameter variation ($h = 0{\cdot}7$ mm), the location where the peak of $\tilde{\beta}_{p_r}$ appears is the same as that for the nominal system, i.e., also at element 8 and $\tilde{\beta}_8 = 1{\cdot}62$;
- the trend of curves for β_{p_r} and $\tilde{\beta}_{p_r}$ shows good correspondence for these two cases, i.e., the detection result obtained from the nominal case is insensitive to the system's parameter variation.

5. CONCLUSIONS

Sensitivity analysis of sensor locations is significant for the vibration control and damage detection of thin-plate systems. This paper investigates these problems systematically. In the case of vibration control, the influence of parameter variation can be eliminated by the robust determination of sensor locations so that the condition $J_p \gg 1$ is satisfied. Among these sensor locations, the OSLs are obtained by minimizing the SCN of Hankel matrix $\mathbf{H}_{k-1}$, which is constructed from the measured data. Using the matrix perturbation theory, the effect of noise on the determination of OSLs is discussed, and the sensitivity of the OSLs to noise depends on the variance of noise and the ranks of $\mathbf{H}_{k-1}$ and $\tilde{\mathbf{H}}_{k-1}$. In the case of damage detection, the index β_{p_r} for nominal cases (or $\tilde{\beta}_{p_r}$ for variational cases), derived from the change of curvature mode shapes, is effective in detecting damage locations. The sensitivity analysis of sensor locations on the detection results for the system with parameter variation is discussed, and the relationship between β_{p_r} and $\tilde{\beta}_{p_r}$ is given. Experimental studies show good agreement with the theoretical analysis.

ACKNOWLEDGMENT

The authors would like to thank the Research Committee of the Hong Kong Polytechnic University for the financial support to this project.

REFERENCES

1. F. E. UDWADIA 1994 *Journal of Engineering Mechanics* **120**, 368–390. Methodology for optimum sensor locations for parameter identification in dynamic systems.
2. P. H. KIRKEAARD *et al.* 1994 *Mechanical Systems and Signal Processing* **8**, 639–647. On the optimal location of sensor for parametric identification of linear structural systems.
3. Y. T. SHIH, A. C. LEE and J. H. CHEN 1998 *Mechanical System and Signal Processing* **12**, 641–659. Sensor and actuator placement for modal identification.
4. T. W. LIM 1993 *International Journal of Analytical and Experimental Modal Analysis* **8**, 1–13. Actuator/sensor placement for modal parameter identification of flexible structures.
5. W. GAWRONSKI 1997 *Journal of Sound and Vibration* **208**, 101–109. Actuator and sensor placement for structural testing and control.
6. A. MACKIEWICZ, J. HOLNICKISZULC and F. LOPEZ ALMANSA 1996 *American Institute of Aeronautics and Astronautics Journal* **34**, 857–859. Optimal sensor location in active control of flexible structures.
7. C. VENKATESAN and A. UDAYASANKAR 1999 *Journal of Aircraft* **36**, 434–442. Selection of sensor locations for active vibration control of helicopter fuselages.

8. R. G. COBB and B. S. LIEBST 1997 *American Institute of Aeronautics and Astronautics Journal* **35**, 369–374. Sensor placement and structural damage identification from minimal sensor information.
9. BASSEVILLE, A. BENVENISTE, G. V. MOUSTAKIDES and A. ROUGEE 1987 *IEEE Transactions on Automatic Control* **AC-32**, 1067–1075. Optimal sensor location for detecting changes in dynamical behaviour.
10. T. EMERSON and M. DEIRDRE 1996 *Journal of Guidance, Control and Dynamics* **19**, 961–963. Optimal sensor placement of large flexible space structures.
11. M. A. HAMDAN and A. H. NAYFEH 1989 *Journal of Guidance, Control and Dynamics* **12**, 421–428. Measures of modal controllability and observability for first- and second-order linear systems.
12. C. KAMMER 1996 *Journal of Guidance Control and Dynamics* **19**, 729–731. Optimal sensor placement for modal identification using system-realization methods.
13. K. B. LIM 1992 *Journal of Guidance, Control and Dynamics* **15**, 49–57. Method for optimal actuator and sensor placement for large flexible structures.
14. C. KAMMER 1992 *Transactions of the American Society for Mechanical Engineers, Journal of Dynamic Systems, Measurement, and Control* **114**, 436–443. Effects of noise on sensor placement for on-orbit modal identification of large space structures.
15. T. D. FADALE, A. V. NENNAROKOMOV and A. F. EMERY 1995 *Journal of Heat Transfer* **117**, 373–379. Two approaches to optimal sensor locations.
16. A. HAC and L. LIU 1993 *Journal of Sound and Vibration* **167**, 239–261. Sensor and actuator location in motion control of flexible structures.
17. KOUGEN MA and ZHONGQUAN GU 1992 *Journal of Vibration and Impact* **4**, 23–28. A robust design method for active control system of structural vibration (in Chinese).
18. R. MARIE and A. K. HISHAM 1998 *Mechanical Systems and Signal Processing* **13**, 297–314. Sensors location for updating problems.
19. C. LIU and F. A. TASKER 1996 *Journal of Guidance, Control and Dynamics* **19**, 1349–1356. Sensor placement for time-domain modal parameter estimation.
20. Y. Y. LI, L. H. YAM, K. T. CHAN and T. P. LEUNG 2000 *Computers and Structures* **75**, 609–617. Robust synthesis of active controller for thin plate systems with parameter uncertainties.
21. W. STEWART and J. G. SUN 1990 *Matrix Perturbation Theory*. Boston, MA: Academic Press.
22. A. S. J. SWAMIDAS and Y. CHEN 1995 *Journal of Sound and Vibration* **186**, 325–343. Monitoring crack growth through change of modal parameters.
23. L. H. YAM, T. P. LEUNG, D. B. LI and K. Z. XUE 1996 *Journal of Sound and Vibration* **192**, 251–260. Theoretical and experimental study of modal strain analysis.
24. R. RUOTOLO and C. SURACE 1997 *Journal of Sound and Vibration* **206**, 567–588. Damage assessment of multiple cracked beams: numerical results and experimental validation.
25. N. K. STUBBS, J. T. KIM and C. R. FARRAR 1995 *Proceedings of* 13*th International Modal analysis Conference*. Field verification of a nondestructive damage location and severity estimation algorithm.
26. M. L. WANG, G. HEO and D. SATPATHI 1998 *Smart Material Structure* **7**, 606–616. A health monitoring system for large structural system.
27. K. PANDEY, M. BISWAS and M. M. SAMMAN 1991 *Journal of Sound and Vibration* **145**, 321–332. Damage detection from changes in curvature mode shapes.
28. W. O. WONG, L. H. YAM, Y. Y. LI, L. Y. LAW and K. T. CHAN 2000 *Journal of Sound and Vibration* **232**, 807–822. Vibration analysis of annular plates using mode subtraction method.
29. Y. Y. LI and L. H. YAM 1999 *Mechanical Systems and Signal Processing* **13**, 667–680. Study on model order determination of thin plate systems with parameter uncertainties.